Stable multiscale Petrov–Galerkin finite element method for high frequency acoustic scattering

Dietmar Gallistl, Daniel Peterseim

Angaben zur Veröffentlichung / Publication details:

Gallistl, Dietmar, and Daniel Peterseim. 2015. "Stable multiscale Petrov–Galerkin finite element method for high frequency acoustic scattering." *Computer Methods in Applied Mechanics and Engineering* 295: 1–17. https://doi.org/10.1016/j.cma.2015.06.017.

Stable Multiscale Petrov-Galerkin Finite Element Method for High Frequency Acoustic Scattering

D. Gallistl* D. Peterseim*

Abstract

We present and analyze a pollution-free Petrov-Galerkin multiscale finite element method for the Helmholtz problem with large wave number κ as a variant of [Peterseim, arXiv:1411.1944, 2014]. We use standard continuous Q_1 finite elements at a coarse discretization scale H as trial functions, whereas the test functions are computed as the solutions of local problems at a finer scale h. The diameter of the support of the test functions behaves like mH for some oversampling parameter m. Provided m is of the order of $\log(\kappa)$ and h is sufficiently small, the resulting method is stable and quasi-optimal in the regime where H is proportional to κ^{-1}. In homogeneous (or more general periodic) media, the fine scale test functions depend only on local mesh-configurations. Therefore, the seemingly high cost for the computation of the test functions can be drastically reduced on structured meshes. We present numerical experiments in two and three space dimensions.

Keywords multiscale method, pollution effect, wave propagation, Helmholtz problem, finite element method

AMS subject classification 35J05, 65N12, 65N15, 65N30

1 Introduction

Standard finite element methods (FEMs) for acoustic wave propagation are well known to exhibit the so-called *pollution effect* [BS00], which means that the stability and convergence of the scheme require a much smaller mesh-size than needed for a meaningful approximation of the wave by finite element functions. For an highly oscillatory wave at wave number κ, the typical requirement for a reasonable representation reads $\kappa H \lesssim 1$ for the mesh-size H, that is some fixed number of elements per wave-length. The standard Galerkin FEM typically requires at least $\kappa^\alpha H \lesssim 1$ where $\alpha > 1$ depends on the method and the stability and regularity properties of the continuous problem. There have been various attempts to reduce or avoid the

*Institut für Numerische Simulation, Universität Bonn, Wegelerstraße 6, D-53115 Bonn, Germany, {gallistl,peterseim}@ins.uni-bonn.de

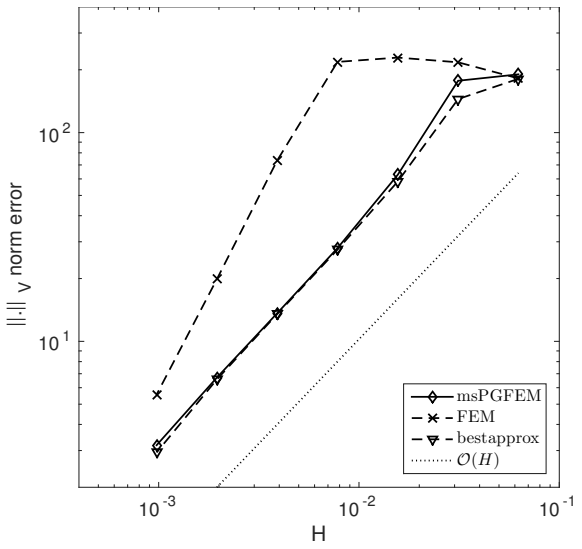

Figure 1: Convergence history of the multiscale FEM (msPGFEM), the standard Q_1 FEM (FEM) and the best-approximation (bestapprox) in the finite element space for a two-dimensional plane wave with wave number $\kappa = 2^7$ (see also Section 5).

pollution effect, e.g., discontinuous Galerkin methods [TF06, FW09, FW11, HMP11], high-order finite elements [MS10, MS11a], discontinuous Petrov-Galerkin methods [ZMD$^+$11, DGMZ12], or the continuous interior penalty method [Wu14] among many others. A good historical overview is provided in [ZMD$^+$11].

The work [Pet14] suggested a multiscale Petrov-Galerkin method for the Helmholtz equation where standard finite element trial and test functions are modified by a local subscale correction in the spirit of numerical homogenization [MP14]. In the numerical experiments of [Pet14], a variant of that method appeared attractive where only the test functions are modified while standard finite element functions are used as trial functions. In this paper, we analyze that method and reformulate it as a stabilized Q_1 method in the spirit of the variational multiscale method [Hug95, HFMQ98, HS07, Mål11, Pet15]. The method employs standard Q_1 finite element trial functions on a grid $\mathcal{G}_H$ with mesh-size H. The test functions are the solutions of local problems with respect to a grid $\mathcal{G}_h$ at a finer scale h which is chosen fine enough to allow for stability of the standard Galerkin FEM over $\mathcal{G}_h$. The diameter of the support of the test functions is proportional to mH for the oversampling parameter m. Under the condition that m is logarithmically coupled with the wave number κ through $m \approx \log(\kappa)$, we prove that the method is pollution-free, i.e., the resolution condition $\kappa H \lesssim 1$ is sufficient for stability and quasi-optimality under fairly general assumptions on the stability of the continuous problem. The performance of the method is illus-

trated in the convergence history of Figure 1. More detailed descriptions on the numerical experiments will be given in Section 5. As the test functions only depend on local mesh-configurations, on structured meshes the number of test functions to be actually computed is much smaller then the overall number of trial and test functions on the coarse scale. In many cases, the computational cost is then dominated by the coarse solve and the overhead compared with a standard FEM on the same coarse mesh remains proportional to $m^d \approx \log(\kappa)^d$. Even if no structure of the mesh can be exploited to reduce the number of patch problems, the method may still be attractive if the problem has to be solved many times with different data (same κ though) in the context of inverse problems or parameter identification problems.

The paper is structured as follows. Section 2 states the Helmholtz problem and recalls some important results. The definition of the new Petrov-Galerkin method follows in Section 3. Stability and error analysis are carried out in Section 4. Section 5 is devoted to numerical experiments.

Standard notation on complex-valued Lebesgue and Sobolev spaces applies throughout this paper. The bar indicates complex conjugation and i is the imaginary unit. The L^2 inner product is denoted by $(v,w)_{L^2(\Omega)} := \int_\Omega v\bar{w}\,dx$. The Sobolev space of complex-valued L^p functions over a domain ω whose generalized derivatives up to order k belong to L^p is denoted by $W^{k,p}(\omega;\mathbb{C})$. The notation $A \lesssim B$ abbreviates $A \leq CB$ for some constant C that is independent of the mesh-size, the wave number κ, and all further parameters in the method like the oversampling parameter m or the fine-scale mesh-size h; $A \approx B$ abbreviates $A \lesssim B \lesssim A$.

2 The Helmholtz Problem

Let $\Omega \subseteq \mathbb{R}^d$, for $d \in \{1,2,3\}$, be an open bounded domain with polyhedral Lipschitz boundary which is decomposed into disjoint parts $\partial\Omega = \Gamma_D \cup \Gamma_R$ with Γ_D closed. The classical Helmholtz equation then reads

$$\begin{aligned} -\Delta u - \kappa^2 u &= f \quad && \text{in } \Omega, \\ u &= u_D && \text{on } \Gamma_D, \\ i\kappa u - \nabla u \cdot \nu &= g && \text{on } \Gamma_R \end{aligned} \tag{2.1}$$

for the outer unit normal ν of Ω and the real parameter $\kappa > 0$. For the sake of a simple exposition we assume $u_D = 0$. Either of the parts Γ_D or Γ_R is allowed to be the empty set. In scattering problems, the Dirichlet boundary Γ_D typically refers to the boundary of a bounded sound-soft object whereas the Robin boundary Γ_R arises from artificially truncating the full space $\mathbb{R}^d$ to the bounded domain Ω [Ihl98]. The variational formulation of (2.1) employs the space

$$V := W^{1,2}_D(\Omega;\mathbb{C}) := \{v \in W^{1,2}(\Omega;\mathbb{C}) \,:\, v|_{\Gamma_D} = 0\}.$$

For any subset $\omega \subseteq \Omega$ we define the norm

$$\|v\|_{V,\omega} := \sqrt{\kappa^2 \|v\|^2_{L^2(\omega)} + \|\nabla v\|^2_{L^2(\omega)}} \quad \text{for any } v \in V$$

and denote $\|v\|_V := \|v\|_{V,\Omega}$. Define on V the following sesquilinear form

$$a(v,w) := (\nabla v, \nabla w)_{L^2(\Omega)} - \kappa^2 (v,w)_{L^2(\Omega)} - i\kappa (v,w)_{L^2(\Gamma_R)}.$$

Although the results of this paper hold for a rather general right-hand side in the dual of V, we focus on data $f \in L^2(\Omega;\mathbb{C})$ and $g \in L^2(\Gamma_R;\mathbb{C})$ for the ease of presentation. The weak form of the Helmholtz problem then seeks $u \in V$ such that

$$a(u,v) = (f,v)_{L^2(\Omega)} + (g,v)_{L^2(\Gamma_R)} \quad \text{for all } v \in V. \tag{2.2}$$

We assume that the problem is polynomially well-posed [EM12] in the sense that there exists some constant $\gamma(\kappa,\Omega)$ which depends polynomially on κ such that

$$\gamma(\kappa,\Omega)^{-1} \leq \inf_{v \in V\setminus\{0\}} \sup_{w \in V\setminus\{0\}} \frac{\Re a(v,w)}{\|v\|_V \|w\|_V}. \tag{2.3}$$

For instance, in the particular case of pure impedance boundary conditions $\partial\Omega = \Gamma_R$, it was proved in [Mel95, CF06] by employing a technique of [MIB96] that $\gamma(\kappa,\Omega) \lesssim \kappa$. Further setups allowing for polynomially well-posedness are described in [Het07, EM12, HMP14b]. In particular, the case of a medium described by a convex domain (with Robin boundary conditions on the outer part of the boundary) and a star-shaped scatterer (with Dirichlet boundary conditions) allows for polynomial well-posedness [Het07]. Another admissible setting is described in [EM12] where Ω is a bounded Lipschitz domain with pure Robin boundary. For general configurations, however, the dependence of the stability constant $\gamma(\kappa,\Omega)$ from (2.3) is an open question. Throughout this paper we assume that (2.3) is satisfied. The case of a possible exponential dependence [BCWG$^+$11] is excluded here.

3 The Method

This section introduces the notation on finite element spaces and meshes and defines the multiscale Petrov-Galerkin method (msPGFEM) for the Helmholtz problem.

3.1 Meshes and Data Structures

Let $\mathcal{G}_H$ be a regular partition of Ω into intervals, parallelograms, parallelepipeds for $d = 1, 2, 3$, respectively, such that $\cup\mathcal{G}_H = \overline{\Omega}$ and any two distinct $T, T' \in \mathcal{G}_H$ are either disjoint or share exactly one lower-dimensional

hyper-face (that is a vertex or an edge for $d \in \{2,3\}$ or a face for $d=3$). We impose shape-regularity in the sense that the aspect ratio of the elements in $\mathcal{G}_H$ is uniformly bounded. Since we are considering quadrilaterals (resp. hexahedra) with parallel faces, this guarantees the non-degeneracy of the elements in $\mathcal{G}_H$. We consider this type of partitions for the sake of a simple presentation and to exploit the structure to increase the computational efficiency. The theory of this paper carries over to simplicial triangulations or to more general quadrilateral or hexahedral partitions satisfying suitable non-degeneracy conditions or even to meshless methods based on proper partitions of unity [HMP14a].

Given any subdomain $S \subseteq \overline{\Omega}$, define its neighbourhood via

$$\mathsf{N}(S) := \operatorname{int}\Big(\cup \{T \in \mathcal{G}_H \,:\, T \cap \overline{S} \neq \emptyset\}\Big).$$

Furthermore, we introduce for any $m \geq 2$ the patches

$$\mathsf{N}^1(S) := \mathsf{N}(S) \qquad \text{and} \qquad \mathsf{N}^m(S) := \mathsf{N}(\mathsf{N}^{m-1}(S)).$$

The shape-regularity implies that there is a uniform bound $C_{\mathrm{ol},m} = C_{\mathrm{ol},m}(d)$ on the number of elements in the mth-order patch,

$$\max_{T \in \mathcal{G}_H} \operatorname{card}\{K \in \mathcal{G}_H \,:\, K \subseteq \overline{\mathsf{N}^m(T)}\} \leq C_{\mathrm{ol},m}.$$

We abbreviate $C_{\mathrm{ol}} := C_{\mathrm{ol},1}$. Throughout this paper, we assume that the coarse-scale mesh $\mathcal{G}_H$ is quasi-uniform. This implies that $C_{\mathrm{ol},m}$ depends polynomially on m. The global mesh-size reads $H := \max\{\operatorname{diam}(T) : T \in \mathcal{G}_H\}$. Let $Q_p(\mathcal{G}_H)$ denote the space of piecewise polynomials of partial degree $\leq p$. The space of globally continuous piecewise first-order polynomials reads

$$\mathcal{S}^1(\mathcal{G}_H) := C^0(\Omega) \cap Q_1(\mathcal{G}_H).$$

The standard Q_1 finite element space reads

$$V_H := \mathcal{S}^1(\mathcal{G}_H) \cap V.$$

The set of free vertices (the degrees of freedom) is denoted by

$$\mathcal{N}_H := \{z \in \overline{\Omega} \,:\, z \text{ is a vertex of } \mathcal{G}_H \text{ and } z \notin \Gamma_D\}.$$

Let $I_H : V \to V_H$ be a surjective quasi-interpolation operator that acts as a stable quasi-local projection in the sense that $I_H \circ I_H = I_H$ and that for any $T \in \mathcal{G}_H$ and all $v \in V$ there holds

$$H^{-1}\|v - I_H v\|_{L^2(T)} + \|\nabla I_H v\|_{L^2(T)} \leq C_{I_H}\|\nabla v\|_{L^2(\mathsf{N}(T))}. \tag{3.1}$$

Under the mesh condition that $\kappa H \lesssim 1$ is bounded by a generic constant, this implies stability in the $\|\cdot\|_V$ norm

$$\|I_H v\|_V \leq C_{I_H,V}\|v\|_V \quad \text{for all } v \in V, \tag{3.2}$$

with a κ-independent constant $C_{I_H,V}$. One possible choice (which we use in our implementation of the method) is to define $I_H := E_H \circ \Pi_H$, where Π_H is the piecewise L^2 projection onto $Q_1(\mathcal{G}_H)$ and E_H is the averaging operator that maps $Q_1(\mathcal{G}_H)$ to V_H by assigning to each free vertex the arithmetic mean of the corresponding function values of the neighbouring cells, that is, for any $v \in Q_1(\mathcal{G}_H)$ and any free vertex $z \in \mathcal{N}_H$,

$$(E_H(v))(z) = \sum_{\substack{T\in\mathcal{G}_H \\ \text{with } z\in T}} v|_T(z) \Big/ \operatorname{card}\{K \in \mathcal{G}_H \,:\, z \in K\}.$$

Note that $E_H(v)|_{\Gamma_D} = 0$ by construction. For this choice, the proof of (3.1) follows from combining the well-established approximation and stability properties of Π_H and E_H, see, e.g., [DE12].

3.2 Definition of the Method

The method is determined by three parameters, namely the coarse-scale mesh-size H, and the stabilization parameters h (the fine-scale mesh-size) and m (the oversampling parameter) which are explained in the following. We assign to any $T \in \mathcal{G}_H$ its m-th order patch $\Omega_T := \mathsf{N}^m(T)$ (for a positive integer m) and define for any $v, w \in V$ the localized sesquilinear forms

$$a_{\Omega_T}(v,w) := (\nabla v, \nabla w)_{L^2(\Omega_T)} - (\kappa^2 v, w)_{L^2(\Omega_T)} - i(\kappa v, w)_{L^2(\Gamma_R \cap \partial\Omega_T)}$$

and

$$a_T(v,w) := (\nabla v, \nabla w)_{L^2(T)} - (\kappa^2 v, w)_{L^2(T)} - i(\kappa v, w)_{L^2(\Gamma_R \cap \partial T)}.$$

Let $\mathcal{G}_h$ be a global uniform refinement of the mesh $\mathcal{G}_H$ over Ω and define

$$V_h(\Omega_T) := \{v \in Q_1(\mathcal{G}_h) \cap V \,:\, v = 0 \text{ outside } \Omega_T\}.$$

Define the null space

$$W_h(\Omega_T) := \{v_h \in V_h(\Omega_T) \,:\, I_H(v_h) = 0\}$$

of the quasi-interpolation operator I_H defined in the previous section. Given any nodal basis function $\Lambda_z \in V_H$, let $\lambda_{z,T} \in W_h(\Omega_T)$ solve the subscale corrector problem

$$a_{\Omega_T}(w, \lambda_{z,T}) = a_T(w, \Lambda_z) \quad \text{for all } w \in W_h(\Omega_T). \tag{3.3}$$

The well-posedness of (3.3) will be proved in Section 4. Let $\lambda_z := \sum_{T\in\mathcal{G}_H} \lambda_{z,T}$ and define the test function

$$\widetilde{\Lambda}_z := \Lambda_z - \lambda_z.$$

The space of test functions then reads

$$\widetilde{V}_H := \operatorname{span}\{\widetilde{\Lambda}_z \,:\, z \in \mathcal{N}_H\}.$$

We emphasize that the dimension $\dim V_H = \dim \widetilde{V}_H$ is independent of the parameters m and h. Figures 2–3 display typical examples for the test functions $\widetilde{\Lambda}_z$ and correctors. The multiscale Petrov-Galerkin FEM seeks $u_H \in V_H$ such that

$$a(u_H, \tilde{v}_H) = (f, \tilde{v}_H)_{L^2(\Omega)} + (g, \tilde{v}_H)_{L^2(\Gamma_R)} \quad \text{for all } \tilde{v}_H \in \widetilde{V}_H. \tag{3.4}$$

The error analysis and the numerical experiments will show that the choice $H \lesssim \kappa^{-1}$, $m \approx \log(\kappa)$ suffices to guarantee stability and quasi-optimality properties, provided that $\kappa^\alpha h \lesssim 1$ where α depends on the stability and regularity of the continuous problem. The conditions on h are the same as for the standard Q_1 FEM on the global fine scale (e.g. $\kappa^{3/2}h \lesssim 1$ for stability [Wu14] and $\kappa^2 h \lesssim 1$ for quasi-optimality [Mel95] in the case of pure Robin boundary conditions on a convex domain).

3.3 Remarks on Generalizations of the Method

The present approach exploits additional structure in the mesh and thereby drastically decreases the cost for the computation of the test functions $(\widetilde{\Lambda}_z : z \in \mathcal{N}_H)$. Indeed, (3.3) is translation-invariant and, thus, the number of corrector problems to be solved is determined by the number of patch configurations. This number is typically much smaller than the number of elements in $\mathcal{G}_H$, see Figure 4 for an illustration.

Some remarks on more general versions of the presented msPGFEM are in order.

Element shapes. As Figure 4 illustrates, highly structured meshes are desirable as they lead to a moderate number of patch problems. The method presented in Subsection 3.2 considers, for simplicity, a partition of the domain in parallelepipeds. While in scattering problems the outer part of the boundary Γ_R results from a truncation of the full space and, hence, the choice of a simple geometry (e.g., a cube) is justified, it is extremely important to guarantee an accurate representation of more general scattering objects. This requires more general element shapes such as isoparametric elements or partitions in bricks and simplices with first-order ansatz functions on the reference cell (see [Pet14] for simplicial meshes). The msPGFEM and its error analysis is also applicable to this situation. The configurations at the boundary will then determine the number of corrector problems.

Fine-scale grid. The present approach is based on a global fine-scale grid $\mathcal{G}_h$ and a particular choice of the domains Ω_T, which is convenient for the

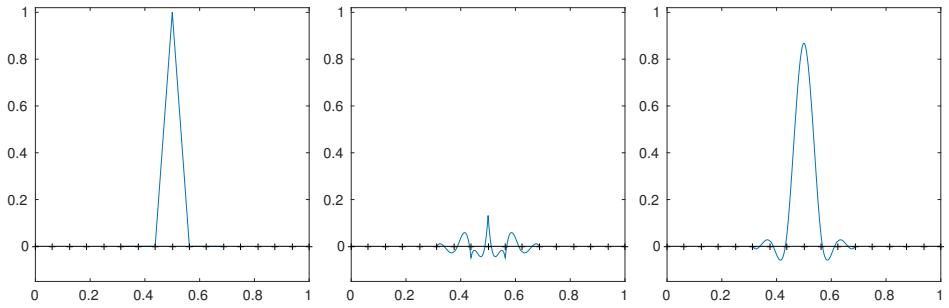

Figure 2: Coarse-scale trial function Λ_z (left), corrector λ_z (middle), and modified test function $\widetilde{\Lambda}_z = \Lambda_z - \lambda_z$ (right) in 1D with $\kappa = 2^5$, $H = 2^{-4}$, $h = 2^{-10}$, $m = 2$.

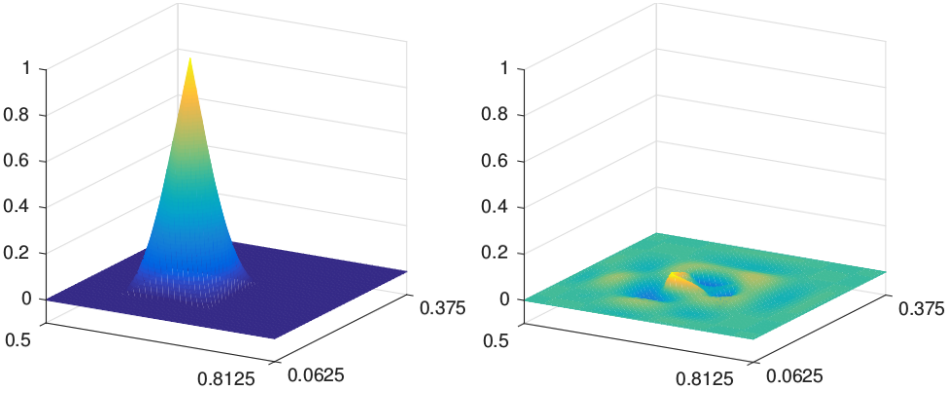

Figure 3: Coarse-scale trial function Λ_z (left), and element corrector $\lambda_{z,T}$ (right) in 2D with $\kappa = 2^5$, $H = 2^{-4}$, $h = 2^{-7}$, $m = 2$ for the patch highlighted in Figure 4.

implementation of the method. It is, however, not necessary for the domains Ω_T to be aligned with the mesh $\mathcal{G}_H$. Also the spaces $W_h(\Omega_T)$ can be defined over independent fine-scale meshes over Ω_T.

Adaptive methods. For certain configurations of the domains Ω_T, for instance in the presence of re-entrant corners, it may be desirable to utilize an adaptive fine-scale mesh over Ω_T for the solution of the corrector problem (3.3). As proven in Lemma 1 below, the corrector problems are coercive and mesh-adaptation may improve the efficiency of the fine-scale corrector problem. As mentioned in the previous remark, it is indeed possible to employ independent fine-scale meshes over different domains Ω_T, Ω_K. The stability and error analysis for the adaptive case, which are expected to be more involved, are not discussed in this paper.

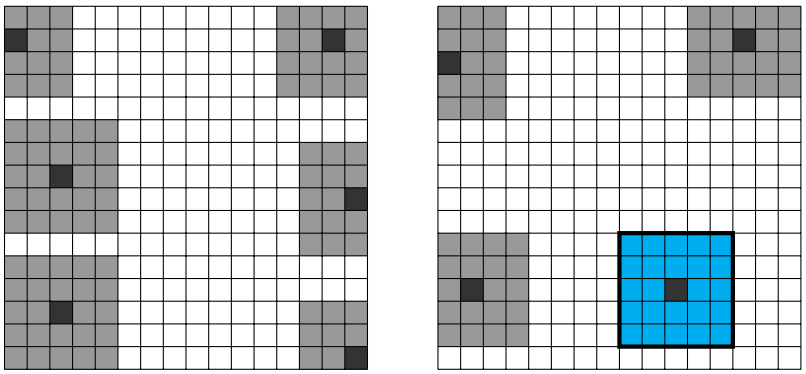

Figure 4: All possible patch configurations (up to rotations) on a structured mesh of the square domain with pure Robin boundary with $m = 2$. A trial function and corresponding corrector for the highlighted patch is depicted in Figure 3.

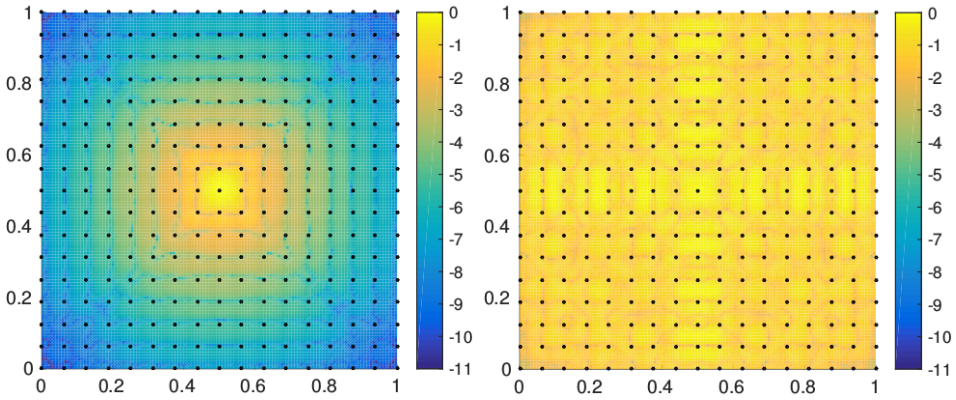

Figure 5: Modulus of the idealized test function $\widetilde{\Lambda}_z$ for $m = \infty$, $H = 2^{-4}$, $h = 2^{-7}$ in 2D in a logarithmically scaled plot. The dots indicate the grid points of the coarse mesh. Left: $\kappa = 2^5$; right: $\kappa = 2^6$.

4 Error Analysis

We denote the global finite element space on the fine scale by $V_h := V_h(\Omega) = \mathcal{S}^1(\mathcal{G}_h) \cap V$. We denote the solution operator of the element corrector problem (3.3) by $\mathcal{C}_{T,m}$. Then any $z \in \mathcal{N}_H$ and any $T \in \mathcal{G}_H$ satisfy $\lambda_{z,T} = \mathcal{C}_{T,m}(\Lambda_z)$ and we refer to $\mathcal{C}_{T,m}$ as element correction operator. The map $\Lambda_z \mapsto \lambda_z$ described in Subsection 3.2 defines a linear operator $\mathcal{C}_m$ via $\mathcal{C}_m(\Lambda_z) = \lambda_z$ for any $z \in \mathcal{N}_H$, referred to as correction operator. For the analysis we introduce idealized counterparts of these correction operators where the patch Ω_T equals Ω. Define the null space space $W_h := \{v \in V_h : I_H(v) = 0\}$. For any $v \in V$, the idealized element corrector problem seeks $\mathcal{C}_{T,\infty} v \in W_h$ such that

$$a(w, \mathcal{C}_{T,\infty} v) = a_T(w, v) \quad \text{for all } w \in W_h. \tag{4.1}$$

Furthermore, define

$$\mathcal{C}_\infty v := \sum_{T \in \mathcal{G}_H} \mathcal{C}_{T,\infty} v. \tag{4.2}$$

It is proved in [MS10, Corollary 3.2] that the form a is continuous and there is a constant C_a such that

$$a(v, w) \leq C_a \|v\|_V \|w\|_V \quad \text{for all } v, w \in V.$$

The following result implies the well-posedness of the idealized corrector problems.

Lemma 1 (well-posedness of the idealized corrector problems)**.** *Provided*

$$C_{I_H} \sqrt{C_{\mathrm{ol}}} H \kappa \leq 1/\sqrt{2}, \tag{4.3}$$

we have for all $w \in W_h$ equivalence of norms

$$\|\nabla w\|_{L^2(\Omega)} \leq \|w\|_V \leq \sqrt{3/2}\, \|\nabla w\|_{L^2(\Omega)}$$

and ellipticity

$$\frac{1}{2} \|\nabla w\|^2_{L^2(\Omega)} \leq \Re a(w, w).$$

Proof. For any $w \in W_h$ the property (3.1) implies

$$\kappa^2 \|w\|^2_{L^2(\Omega)} = \kappa^2 \|(1 - I_H) w\|^2_{L^2(\Omega)} \leq C^2_{I_H} C_{\mathrm{ol}} H^2 \kappa^2 \|\nabla w\|^2_{L^2(\Omega)}. \qquad \square$$

Lemma 1 implies that the idealized corrector problems (4.2) are well-posed and the correction operator $\mathcal{C}_\infty$ is continuous in the sense that

$$\|\mathcal{C}_\infty v_H\|_V \leq C_{\mathcal{C}} \|v_H\|_V \quad \text{for all } v_H \in V_H$$

for some constant $C_{\mathcal{C}} \approx 1$. Since the inclusion $W_h(\Omega_T) \subseteq W_h$ holds, the well-posedness result of Lemma 1 carries over to the corrector problems (3.3) in the subspace $W_h(\Omega_T)$ with the sesquilinear form a_{Ω_T}.

The proof of well-posedness of the Petrov-Galerkin method (3.4) will be based on the fact that the difference $(\mathcal{C}_\infty - \mathcal{C}_m)(v)$ decays exponentially with the distance from $\operatorname{supp}(v)$. In the next theorem, we quantify the difference between the idealized and the discrete correctors. The proof will be given in Appendix A of this paper and is based on the exponential decay of the corrector $\mathcal{C}_\infty \Lambda_z$ itself, see Figure 5. That figure also illustrates that the decay requires the resolution condition (4.3), namely $\kappa H \lesssim 1$.

Theorem 1. *Under the resolution condition* (4.3) *there exist constants* $C_1 \approx 1 \approx C_2$ *and* $0 < \beta < 1$ *such that any* $v \in V_H$*, any* $T \in \mathcal{G}_H$ *and any* $m \in \mathbb{N}$ *satisfy*

$$\|\nabla(\mathcal{C}_{T,\infty} v - \mathcal{C}_{T,m} v)\|_{L^2(\Omega)} \leq C_1 \beta^m \|\nabla v\|_{L^2(T)}, \tag{4.4}$$

$$\|\nabla(\mathcal{C}_\infty v - \mathcal{C}_m v)\|_{L^2(\Omega)} \leq C_2 \sqrt{C_{\mathrm{ol},m}} \beta^m \|\nabla v\|_{L^2(\Omega)}. \tag{4.5}$$

□

Provided h is chosen fine enough, the standard FEM over $\mathcal{G}_h$ is stable in the sense that there exists a constant C_{FEM} such that with $\gamma(\kappa, \Omega)$ from (2.3) there holds

$$\big(C_{\mathrm{FEM}} \gamma(\kappa, \Omega)\big)^{-1} \leq \inf_{v \in V_h \setminus \{0\}} \sup_{w \in V_h \setminus \{0\}} \frac{\Re a(v, w)}{\|v\|_V \|w\|_V}. \tag{4.6}$$

This is actually a condition on the fine-scale parameter h. In general, the requirements on h depend on the stability of the continuous problem [Mel95].

Theorem 2 (well-posedness of the discrete problem)**.** *Under the resolution conditions* (4.3) *and* (4.6) *and the following oversampling condition*

$$m \geq |\log\big(\sqrt{6} C_a \sqrt{C_{\mathrm{ol}}} C_{I_H} C_{I_H,V} C_2 \sqrt{C_{\mathrm{ol},m}} C_{\mathrm{FEM}} \gamma(\kappa, \Omega)\big)| \Big/ |\log(\beta)|, \tag{4.7}$$

problem (3.4) *is well-posed and the constant* $C_{\mathrm{PG}} := 2 C_{I_H,V} C_{\mathcal{C}} C_{\mathrm{FEM}}$ *satisfies*

$$\big(C_{\mathrm{PG}} \gamma(\kappa, \Omega)\big)^{-1} \leq \inf_{v_H \in V_H \setminus \{0\}} \sup_{\tilde{v}_H \in \widetilde{V}_H \setminus \{0\}} \frac{\Re a(v_H, \tilde{v}_H)}{\|v_H\|_V \|\tilde{v}_H\|_V}.$$

Proof. Let $u_H \in V_H$ with $\|u_H\|_V = 1$. From (4.6) we infer that there exists some $v \in V_h$ with $\|v\|_V = 1$ such that

$$\Re a(u_H - \overline{\mathcal{C}_\infty(\bar{u}_H)}, v) \geq \big(C_{\mathrm{FEM}} \gamma(\kappa, \Omega)\big)^{-1} \|u_H - \overline{\mathcal{C}_\infty(\bar{u}_H)}\|_V.$$

It follows from the structure of the sesquilinear form a that $\overline{\mathcal{C}_\infty(\bar{u}_H)}$ solves the following adjoint corrector problem

$$a(\overline{\mathcal{C}_\infty(\bar{u}_H)}, w) = a(u_H, w) \quad \text{for all } w \in W_h, \tag{4.8}$$

cf. [MS11b, Lemma 3.1]. Let $\tilde{v}_H := (1 - \mathcal{C}_m) I_H v \in \widetilde{V}_H$. We have

$$a(u_H, \tilde{v}_H) = a(u_H, (1 - \mathcal{C}_\infty) I_H v) + a(u_H, (\mathcal{C}_\infty - \mathcal{C}_m) I_H v). \tag{4.9}$$

Since $\mathcal{C}_\infty$ is a projection onto W_h, we have $(1 - \mathcal{C}_\infty)(1 - I_H)v = 0$ and, thus, $(1 - \mathcal{C}_\infty) I_H v = (1 - \mathcal{C}_\infty) v$. The solution properties (4.8) of $\overline{\mathcal{C}_\infty(\bar{u}_H)}$ and (4.1)–(4.2) of $\mathcal{C}_\infty v$ prove $a(u_H, \mathcal{C}_\infty v) = a(\overline{\mathcal{C}_\infty(\bar{u}_H)}, v)$. Hence,

$$\begin{aligned} \Re a(u_H, (1 - \mathcal{C}_\infty) I_H v) &= \Re a(u_H - \overline{\mathcal{C}_\infty(\bar{u}_H)}, v) \\ &\geq \left(C_{\mathrm{FEM}} \gamma(\kappa, \Omega)\right)^{-1} \|u_H - \overline{\mathcal{C}_\infty(\bar{u}_H)}\|_V. \end{aligned}$$

Furthermore, the estimate (3.2) implies

$$1 = \|u_H\|_V = \|I_H(u_H - \overline{\mathcal{C}_\infty(\bar{u}_H)})\|_V \leq C_{I_H,V} \|u_H - \overline{\mathcal{C}_\infty(\bar{u}_H)}\|_V.$$

The second term on the right-hand side of (4.9) satisfies with $\|u_H\|_V = 1$ and Lemma 1 that

$$|a(u_H, (\mathcal{C}_\infty - \mathcal{C}_m) I_H v)| \leq \sqrt{3/2} C_a \|\nabla (\mathcal{C}_\infty - \mathcal{C}_m) I_H v\|_{L^2(\Omega)}.$$

Altogether, it follows that

$$\Re a(u_H, \tilde{v}_H) \geq \left(\frac{1}{C_{I_H,V} C_{\mathrm{FEM}} \gamma(\kappa, \Omega)} - \sqrt{\frac{3}{2}} C_a \|\nabla (\mathcal{C}_\infty - \mathcal{C}_m) I_H v\|_{L^2(\Omega)} \right).$$

Theorem 1 and (3.1) show that

$$\|\nabla (\mathcal{C}_\infty - \mathcal{C}_m) I_H v\|_{L^2(\Omega)} \leq C_2 \sqrt{C_{\mathrm{ol},m}} \beta^m \|\nabla I_H v\| \leq C_2 \sqrt{C_{\mathrm{ol},m}} C_{I_H} \sqrt{C_{\mathrm{ol}}} \beta^m.$$

Hence, the condition (4.7) and $\|\tilde{v}_H\|_V = \|(1 - \mathcal{C}_\infty) v\|_V \leq C_{\mathcal{C}}$ imply the assertion. □

Remark 1 (adjoint problem)**.** *Under the assumptions of Theorem 2, problem* (3.4) *is well-posed and, thus, it follows from a dimension argument that there is non-degeneracy of the sesquilinear form a over $V_H \times \widetilde{V}_H$. Thus, the adjoint problem to* (3.4) *is well-posed with the same stability constant as in Theorem 2.*

The quasi-optimality result requires the following additional condition on the oversampling parameter m,

$$m \geq |\log\left(2 C_2 \sqrt{C_{\mathrm{ol},m}} C_a^2 C_{\mathrm{PG}} \gamma(\kappa, \Omega) \sqrt{3/2}\right)| \Big/ |\log(\beta)|. \tag{4.10}$$

Theorem 3 (quasi-optimality)**.** *The resolution conditions* (4.3) *and* (4.6) *and the oversampling conditions* (4.7) *and* (4.10) *imply that the solution u_H to* (3.4) *with parameters H, h, and m and the solution u_h of the standard Galerkin FEM on the mesh $\mathcal{G}_h$ satisfy*

$$\|u_h - u_H\|_V \lesssim \|(1 - I_H) u_h\|_V \approx \min_{v_H \in V_H} \|u_h - v_H\|_V.$$

Proof. Let $e := u_h - u_H$. The triangle inequality and Lemma 1 yield

$$\|e\|_V \leq \|(1 - I_H)u_h\|_V + \|I_H e\|_V.$$

It remains to bound the second term on the right-hand side. The proof employs a standard duality argument, the stability of the idealized method and the fact that our practical method is a perturbation of that ideal method. Let $z_H \in V_H$ be the solution to the dual problem

$$(\nabla v_H, \nabla I_H e) + \kappa^2 (v_H, I_H e) = a(v_H, (1 - \mathcal{C}_\infty) z_H)$$

for all $v_H \in V_H$ (cf. Remark 1). The choice of the test function $v_H = I_H e$ implies that

$$\|I_H e\|_V^2 = a(I_H e, (1-\mathcal{C}_\infty) z_H) = a(I_H e, (\mathcal{C}_m - \mathcal{C}_\infty) z_H) + a(I_H e, (1-\mathcal{C}_m) z_H).$$

The identity $I_H(\mathcal{C}_m - \mathcal{C}_\infty) z_H = 0$, the resolution condition (4.3), the estimate (4.5), and the stability of the adjoint problem imply for the first term on the right-hand side that

$$\begin{aligned}
&a(I_H e, (\mathcal{C}_m - \mathcal{C}_\infty) z_H) \\
&\leq C_a \sqrt{3/2} \|I_H e\|_V \|\nabla (\mathcal{C}_m - \mathcal{C}_\infty) z_H\|_{L^2(\Omega)} \\
&\leq C_2 \sqrt{C_{\mathrm{ol},m}} C_a \sqrt{3/2} \|I_H e\|_V \beta^m \|\nabla z_H\| \\
&\leq C_2 \sqrt{C_{\mathrm{ol},m}} C_a^2 C_{\mathrm{PG}} \gamma(\kappa, \Omega) \sqrt{3/2} \beta^m \|I_H e\|_V^2.
\end{aligned}$$

The condition (4.10) implies that this is $\leq \frac{1}{2} \|I_H e\|_V^2$. The Galerkin orthogonality $a(u_h - u_H, (1 - \mathcal{C}_m) z_H) = 0$, the solution property (4.2) of $\mathcal{C}_\infty z_H$, the resolution condition (4.3) and the exponential decay (4.5) imply for the second term

$$\begin{aligned}
a(I_H e, (1 - \mathcal{C}_m) z_H) &= a(I_H u_h - u_h, (1 - \mathcal{C}_m) z_H) \\
&= a(I_H u_h - u_h, (\mathcal{C}_\infty - \mathcal{C}_m) z_H) \\
&\leq \sqrt{3/2} C_a C_2 \sqrt{C_{\mathrm{ol},m}} \beta^m \|I_H u_h - u_h\|_V \|\nabla z_H\|_{L^2(\Omega)}.
\end{aligned}$$

The stability of the adjoint problem implies

$$\|\nabla z_H\|_{L^2(\Omega)} \leq C_{\mathrm{PG}} \gamma(\kappa, \Omega) C_a \|I_H e\|_V.$$

Thus,

$$a(I_H e, (1-\mathcal{C}_m) z_H) \leq \sqrt{3/2} C_a^2 C_2 \sqrt{C_{\mathrm{ol},m}} C_{\mathrm{PG}} \beta^m \gamma(\kappa, \Omega) \|I_H u_h - u_h\|_V \|I_H e\|_V.$$

The term $\|I_H e\|_V$ can be absorbed and the oversampling condition (4.7) implies that $\beta^m \sqrt{C_{\mathrm{ol},m}} \gamma(\kappa, \Omega)$ is controlled by some κ-independent constant. The combination with the foregoing displayed formulae concludes the proof. □

The following consequence of Theorem 3 states an estimate for the error $u - u_H$.

Corollary 1. *Under the conditions of Theorem 3, the discrete solution u_H to* (3.4) *satisfies with some constant $C \approx 1$ that*

$$\|u - u_H\|_V \leq \|u - u_h\|_V + C \min_{v_H \in V_H} \|u_h - v_H\|_V.$$

In particular, provided that the solution satisfies $u \in W^{1,s}(\Omega)$ for $0 < s \leq 1$, the error decays as $\|u - u_H\|_V \leq \mathcal{O}(H^s)$. □

Remark 2. *In the idealized case that $m = \infty$, we have $u_h - I_H u_h \in W_h$ and, thus,*

$$a(u_h - I_H u_h, (1 - \mathcal{C}_\infty)v_H) = 0 \quad \text{for all } v_H \in V_H.$$

Therefore, problem (3.4) *and the Galerkin property show that $u_H = I_H u_h$.*

5 Numerical Experiments

We investigate the method in three numerical experiments. The convergence history plots display the absolute error in the norm $\|\cdot\|_V$ versus the mesh size H.

5.1 Plane Wave on the Square Domain

On the unit square $\Omega = (0,1)^2$, we consider the pure Robin problem $\Gamma_R = \partial\Omega$ with data given by the plane wave $u(x) = \exp(-i\kappa x \cdot \binom{0.6}{0.8})$.

Figure 6a–6c displays the convergence history for $\kappa = 2^6, 2^7, 2^8$ and the fine-scale mesh parameter $h = 2^{-11}$. The best-approximation error of continuous Q_1 functions in $\|\cdot\|_V$ and the error of the standard Galerkin FEM on the same coarse mesh are plotted for comparison. As expected, the standard FEM clearly exhibits the pollution effect, and larger values of κ increase the discrepancy between the approximation error of the FEM and the theoretical best-approximation by Q_1 functions in the regime under consideration. In contrast, the approximation by the msPGFEM can compete with the best-approximation on meshes that allow a meaningful representation of the solution. We stress the fact that the convergence history plots merely take into account the coarse mesh-size H, but the computational cost in the multiscale method is moderately higher than in the standard FEM due to the increased communication caused by the coupling $m \approx \log(\kappa)$.

For the oversampling parameter $m = 2$, the number of corrector problems to be solved for the finest mesh $\mathcal{G}_H$ is 49 out of 1 048 576 when no symmetry is exploited.

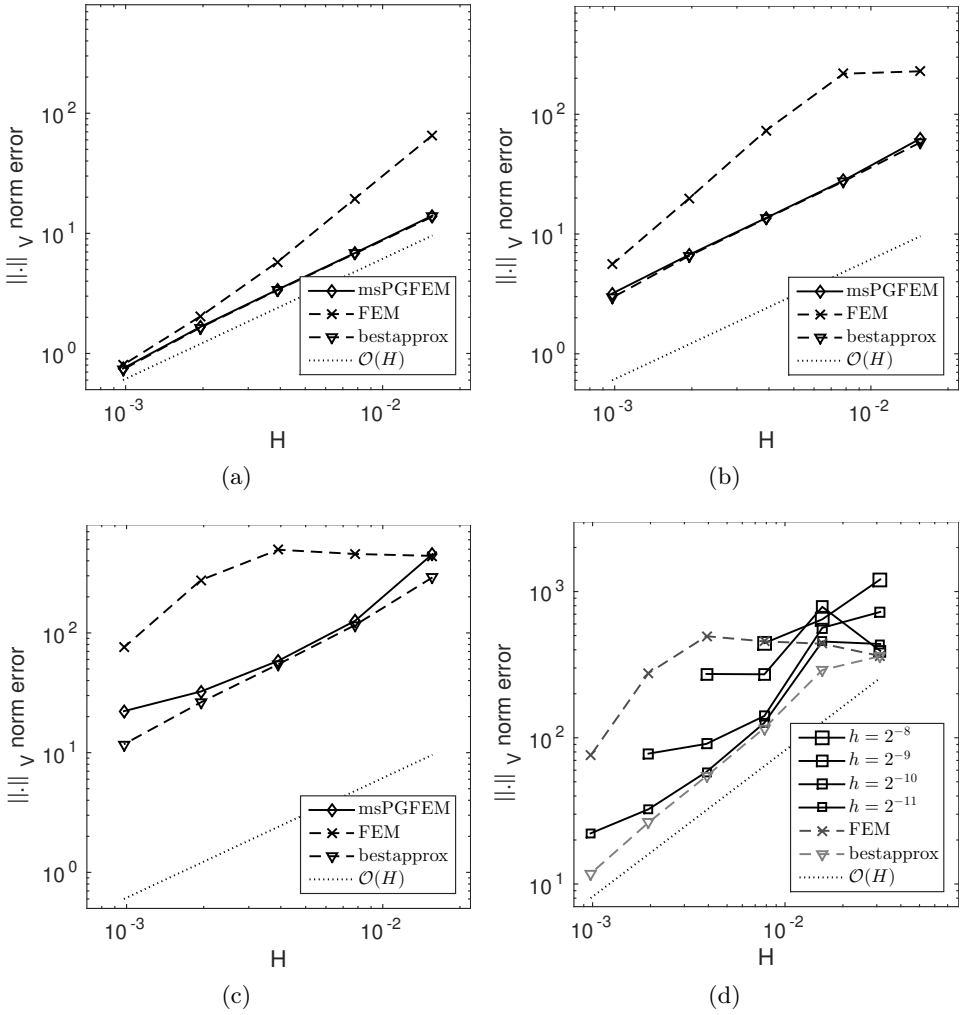

Figure 6: (a)–(c). Comparison of the msPGFEM with the best approximation in $\|\cdot\|_V$ and the standard Galerkin FEM for the 2D plane wave example for $\kappa = 2^6, 2^7, 2^8$. (d). Dependence on the fine mesh parameter h in the 2D plane wave example with $\kappa = 2^8$.

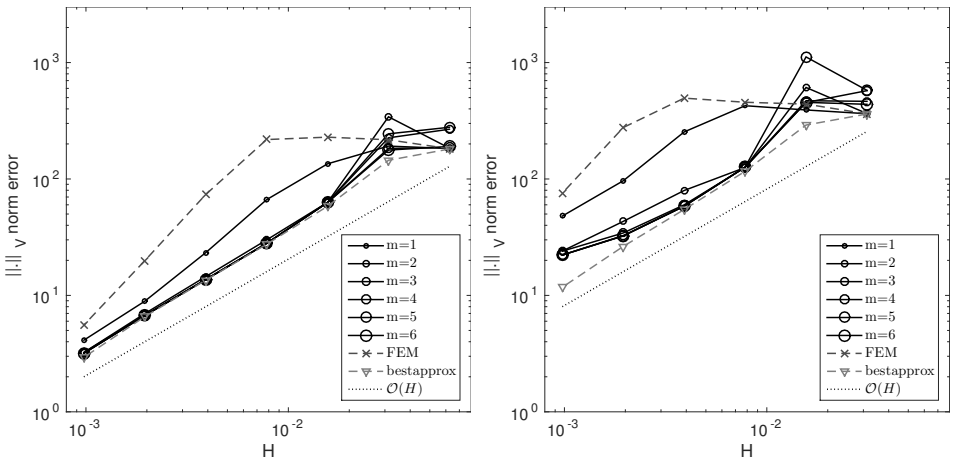

Figure 7: Convergence history for the 2D plane wave example with $\kappa = 2^7$ (left) and $\kappa = 2^8$(right), $h = 2^{-11}$ and varying m.

Figure 6d displays the dependence on the fine mesh parameter h for $\kappa = 2^8$ and oversampling parameter $m = 6$. Since the multiscale method based on the fine grid $\mathcal{G}_h$ computes approximations of the FEM solution on that fine grid, e.g. $u_H = I_H u_h$ for $m = \infty$ as in Remark 2, it is clear that the accuracy of the msPGFEM is limited by the accuracy of the standard FEM on the fine scale. This can be observed in Figure 6d. It can be also seen that a finer fine-scale mesh-size h improves the error of the msPGFEM towards the best-approximation. In this two-dimensional example, the quasi-optimality constant appears to be close to 1

Next, we study the dependence on the oversampling parameter m. Figure 7 displays the convergence history for $\kappa = 2^7$ and $\kappa = 2^8$. The fine mesh parameter is $h = 2^{-11}$ and m varies from $m = 1$ to $m = 6$. It turns out that for the present configuration, the value $m = 2$ is sufficient for quasi-optimality. In the range where H is significantly larger than κ^{-1} and the resolution condition is violated, larger oversampling parameters may lead to larger errors, which is not surprising in view of the lack of decay, see also Figure 5. This, however, is no more the case as soon as H is small enough to allow for a meaningful representation of the wave.

5.2 Multiple Sound-Soft Scatterers in 2D

We consider the domain

$$\Omega := (0,1)^2 \setminus \big(\left[\tfrac{5}{16}, \tfrac{7}{16}\right] \times \left[\tfrac{5}{16}, \tfrac{7}{16}\right] \cup \left[\tfrac{10}{16}, \tfrac{12}{16}\right] \times \left[\tfrac{8}{16}, \tfrac{10}{16}\right] \cup \left[\tfrac{4}{16}, \tfrac{6}{16}\right] \times \left[\tfrac{10}{16}, \tfrac{13}{16}\right] \big)$$

from Figure 8. The incident wave $u_{\text{in}}(x) = \exp(-i\kappa x \cdot \binom{0.6}{0.8})$ is incorporated through the Robin boundary condition with $g := i\kappa u_{\text{in}} + \partial_\nu u_{\text{in}}$ on the outer

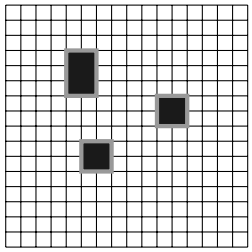

Figure 8: Coarse mesh for the square domain with three scatterers from Subsection 5.2

boundary $\Gamma_R := \{x \in \{0,1\} \text{ or } y \in \{0,1\}\}$. On the remaining part of the boundary $\Gamma_D := \partial\Omega \setminus \Gamma_R$ we impose homogeneous Dirichlet conditions. We choose the fine mesh parameter as $h = 2^{-11}$. Since the exact solution is unknown, we compute a reference solution with the standard Q_1 FEM on the fine mesh $\mathcal{G}_h$ and we compare the coarse approximation with this reference solution. Errors committed by the fine scale are not included in the discussion. Figure 9 displays the convergence history for $\kappa = 2^5$ and $\kappa = 2^6$. The oversampling parameter m varies from $m = 1$ to $m = 4$. As in the foregoing example, the value $m = 2$ for the oversampling parameter seems to be sufficient for the quasi-optimality and even a quasi-optimality constant close to 1 in the range of wave numbers considered here. In particular, the pollution effect that is visible for the standard Galerkin FEM is not present for the msPGFEM. Reduced convergences rates which are expected from the presence of re-entrant corners are not visible in this computational range. For the oversampling parameter $m = 2$, the number of corrector problems to be solved for the finest mesh $\mathcal{G}_H$ is 210 out of 61 952 when no symmetry is exploited.

5.3 Plane Wave on the Cube Domain

On the unit cube $\Omega = (0,1)^3$, we consider the pure Robin problem with data given by the plane wave $u(x) = \exp(-i\kappa x \cdot \frac{1}{\sqrt{38}} \begin{pmatrix} 2 \\ 3 \\ 5 \end{pmatrix})$.

We choose $\kappa = 2^5$. Figure 10 compares the error of the msPGGEM $h = 2^{-4}$ and $m \in \{1,2,3,4\}$ with the best-approximation in the $\|\cdot\|_V$ norm and the error of the standard Galerkin FEM. Also in this example, the msPGFEM is pollution-free for the oversampling parameter $m \geq 2$. The quasi-optimality constant appears slightly larger than in 2D. For the oversampling parameter $m = 2$, the number of corrector problems to be solved for the finest mesh $\mathcal{G}_H$ is 343 out of 262 144 when no symmetry is exploited.

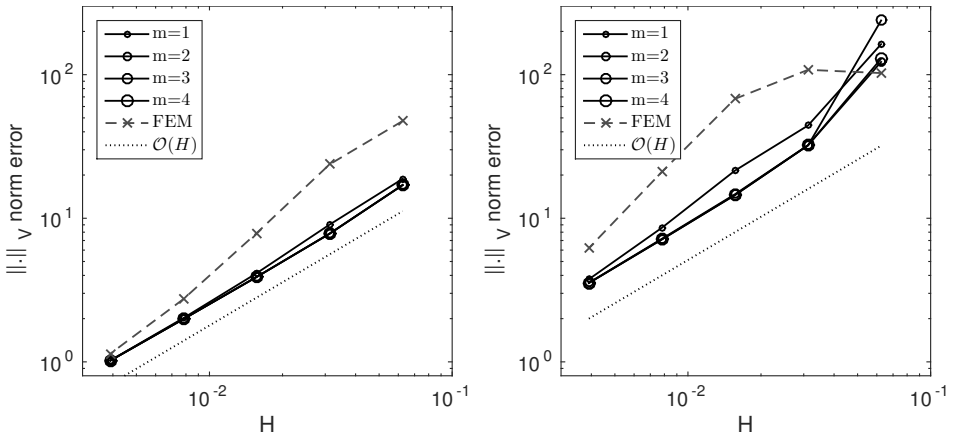

Figure 9: Convergence history for the multiple scattering example from Subsection 5.2 for $\kappa = 2^5$ (left) and $\kappa = 2^6$ (right) $h = 2^{-11}$.

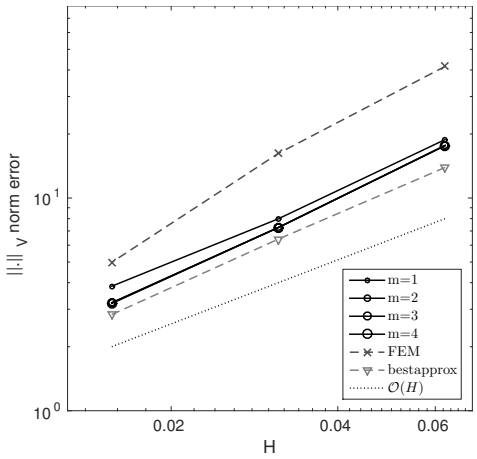

Figure 10: Convergence history for the 3D plane wave example for $\kappa = 2^5$ and $h = 2^{-7}$.

A Appendix: Proof of Theorem 1

For the sake of completeness we also present a proof of the exponential decay result Theorem 4 which is central for the method. The idea of the proof is the same as in the previous proofs of the exponential decay [MP14, HP13, EGMP13, HMP14a, BP14] in the context of diffusion problems. The difference especially with respect to [Pet14] is that here the quasi-interpolation is a projection. This simplifies the proofs and leads to slightly better rates in the exponential decay that have been experimentally observed in [Pet14].

Let $I_h : C^0(\Omega) \to V_h$ denote the nodal Q_1 interpolation operator. Standard interpolation estimates and the inverse inequality prove for any $T \in \mathcal{G}_H$ and all $q \in Q_2(T)$ the stability estimate

$$\|\nabla I_h q\|_{L^2(T)} \leq C_{I_h} \|\nabla q\|_{L^2(T)}. \tag{A.1}$$

In the proofs we will frequently make use of cut-off functions. We collect some properties in the following lemma.

Lemma 2. *Let $\eta \in \mathcal{S}^1(\mathcal{G}_H)$ be a function with values in the interval $[0,1]$ satisfying the bound*

$$\|\nabla \eta\|_{L^\infty(\Omega)} \leq C_\eta H^{-1} \tag{A.2}$$

and let $\mathcal{R} := \operatorname{supp}(\nabla \eta)$. Given any subset $\mathcal{K} \subseteq \mathcal{G}_H$, any $\phi \in W_h$ satisfies for $S = \cup \mathcal{K} \subseteq \overline{\Omega}$ that

$$\|\phi\|_{L^2(S)} \lesssim H \|\nabla \phi\|_{L^2(\mathsf{N}(S))} \tag{A.3}$$

$$\|(1 - I_H) I_h(\eta \phi)\|_{L^2(S)} \lesssim H \|\nabla(\eta \phi)\|_{L^2(\mathsf{N}(S))} \tag{A.4}$$

$$\|\nabla(\eta \phi)\|_{L^2(S)} \lesssim \|\nabla \phi\|_{L^2(S \cap \{\operatorname{supp}(\eta)\})} + \|\nabla \phi\|_{L^2(\mathsf{N}(S \cap \mathcal{R}))}. \tag{A.5}$$

Proof. The property (3.1) readily implies (A.3). Furthermore, (3.1) implies

$$\|(1 - I_H) I_h(\eta \phi)\|_{L^2(S)} \leq H C_{I_H} \sqrt{C_{\mathrm{ol}}} \|\nabla I_h(\eta \phi)\|_{L^2(\mathsf{N}(S))}.$$

Estimate (A.1) leads to

$$\|\nabla I_h(\eta \phi)\|_{L^2(\mathsf{N}(S))} \leq C_{I_h} \|\nabla(\eta \phi)\|_{L^2(\mathsf{N}(S))}.$$

This proves (A.4). For the proof of (A.5) the product rule and (A.2) imply

$$\|\nabla(\eta \phi)\|_{L^2(S)} \leq \|\nabla \phi\|_{L^2(S \cap \{\operatorname{supp}(\eta)\})} + C_\eta H^{-1} \|\phi\|_{L^2(S \cap \mathcal{R})}.$$

The combination with (A.3) concludes the proof. □

Theorem 4 (decay)**.** *Under the resolution condition* (4.3)*, there exists $0 < \beta < 1$ such that, for any $v_H \in V_H$ and all $T \in \mathcal{G}_H$ and $m \in \mathbb{N}$,*

$$\|\nabla \mathcal{C}_{T,\infty} v_H\|_{L^2(\Omega \setminus \mathsf{N}^m(T))} \leq C \beta^m \|\nabla v_H\|_{L^2(T)}.$$

Proof. We define the cut-off function $\eta \in \mathcal{S}^1(\mathcal{G}_H)$ via

$$\eta \equiv 0 \quad \text{in } \mathsf{N}^{m-3}(T) \qquad \text{and} \qquad \eta \equiv 1 \quad \text{in } \Omega \setminus \mathsf{N}^{m-2}(T).$$

Note that η is thereby also uniquely defined on the set $\mathcal{R} := \operatorname{supp}(\nabla\eta)$. The shape-regularity implies that η satisfies (A.2). Let $v_H \in V_H$ and denote $\phi := \mathcal{C}_{T,\infty} v_H \in W_h$. Elementary estimates lead to

$$\begin{aligned}\|\nabla\phi\|^2_{\Omega\setminus\mathsf{N}^m(T)} \leq |(\nabla\phi, \eta\nabla\phi)_{L^2(\Omega)}| &\leq |(\nabla\phi, \nabla(\eta\phi))_{L^2(\Omega)}| + |(\nabla\phi, \phi\nabla\eta)_{L^2(\Omega)}| \\ &\leq M_1 + M_2 + M_3 + M_4\end{aligned}$$

for

$$\begin{aligned} M_1 &:= |(\nabla\phi, \nabla((1-I_h)(\eta\phi)))_{L^2(\Omega)}| & M_2 &:= |(\nabla\phi, \nabla((1-I_H)I_h(\eta\phi)))_{L^2(\Omega)}| \\ M_3 &:= |(\nabla\phi, \nabla(I_H I_h(\eta\phi)))_{L^2(\Omega)}| & M_4 &:= |(\nabla\phi, \phi\nabla\eta)_{L^2(\Omega)}|. \end{aligned}$$

The property (A.1) proves

$$M_1 \leq \|\nabla\phi\|_{L^2(\mathcal{R})} \|\nabla(\eta\phi - I_h(\eta\phi))\|_{L^2(\mathcal{R})} \lesssim \|\nabla\phi\|_{L^2(\mathcal{R})} \|\nabla(\eta\phi)\|_{L^2(\mathcal{R})}.$$

Hence, it follows with (A.5) that

$$M_1 \lesssim \|\nabla\phi\|_{L^2(\mathcal{R})} \|\nabla\phi\|_{L^2(\mathsf{N}(\mathcal{R}))}.$$

Since $w := (1-I_H)I_h(\eta\phi) \in W_h$, the identity (4.1) and the fact that the support of w lies outside T imply $a(w,\phi) = a_T(w, v_H) = 0$ and therefore

$$M_2 = a(w,\phi) + \kappa^2(w,\phi) = \kappa^2(w,\phi) \leq \kappa^2 \|w\|_{L^2(\mathsf{N}(\mathcal{R}))} \|\phi\|_{L^2(\mathsf{N}(\mathcal{R}))}.$$

The estimates (A.3) and (A.4) and the resolution condition $\kappa H \lesssim 1$ from (4.3) imply

$$M_2 \lesssim \|\nabla\phi\|_{L^2(\mathsf{N}^2(\mathcal{R}))} \|\nabla(\eta\phi)\|_{L^2(\mathsf{N}^2(\mathcal{R}))}.$$

The application of (A.5) yields

$$M_2 \lesssim \|\nabla\phi\|_{L^2(\mathsf{N}^2(\mathcal{R}))} (\|\nabla\phi\|_{L^2(\mathsf{N}^2(\mathcal{R}))} + \|\nabla\phi\|_{L^2(\mathsf{N}(\mathcal{R}))}) \lesssim \|\nabla\phi\|^2_{L^2(\mathsf{N}^2(\mathcal{R}))}.$$

The function $I_H I_h(\eta\phi)$ vanishes outside $\mathsf{N}(\mathcal{R})$. Hence, the stability and approximation properties (3.1) and (A.1) lead to

$$\begin{aligned} M_3 &\leq \|\nabla\phi\|_{L^2(\mathsf{N}(\mathcal{R}))} \|\nabla(I_H I_h(\eta\phi))\|_{L^2(\mathsf{N}(\mathcal{R}))} \\ &\lesssim \|\nabla\phi\|_{L^2(\mathsf{N}(\mathcal{R}))} \|\nabla(\eta\phi)\|_{L^2(\mathsf{N}^2(\mathcal{R}))}. \end{aligned}$$

With (A.5) we obtain

$$M_3 \lesssim \|\nabla\phi\|_{L^2(\mathsf{N}(\mathcal{R}))} (\|\nabla\phi\|_{L^2(\mathsf{N}^2(\mathcal{R}))} + \|\nabla\phi\|_{L^2(\mathsf{N}(\mathcal{R}))}) \lesssim \|\nabla\phi\|^2_{L^2(\mathsf{N}^2(\mathcal{R}))}.$$

For the term M_4, the Lipschitz bound (A.2) and (A.3) prove

$$M_4 \leq \|\nabla\phi\|_{L^2(\mathcal{R})}\,\|\phi\|_{L^2(\mathcal{R})}C_\eta H^{-1} \lesssim \|\nabla\phi\|^2_{L^2(\mathsf{N}(\mathcal{R}))}.$$

Altogether, it follows for some constant $\widetilde{C}$ that

$$\|\nabla\phi\|^2_{L^2(\Omega\setminus\mathsf{N}^m(T))} \leq \widetilde{C}\|\nabla\phi\|^2_{L^2(\mathsf{N}^2(\mathcal{R}))}.$$

Recall that $\mathsf{N}^2(\mathcal{R}) = \mathsf{N}^m(T)\setminus\mathsf{N}^{m-5}(T)$. Since

$$\|\nabla\phi\|^2_{L^2(\Omega\setminus\mathsf{N}^m(T))} + \|\nabla\phi\|^2_{L^2(\mathsf{N}^m(T)\setminus\mathsf{N}^{m-5}(T))} = \|\nabla\phi\|^2_{L^2(\Omega\setminus\mathsf{N}^{m-5}(T))},$$

we obtain

$$(1+\widetilde{C}^{-1})\|\nabla\phi\|^2_{L^2(\Omega\setminus\mathsf{N}^m(T))} \leq \|\nabla\phi\|^2_{L^2(\Omega\setminus\mathsf{N}^{m-5}(T))}.$$

The repeated application of this argument proves for $\tilde{\beta} := (1+\widetilde{C}^{-1})^{-1} < 1$ that

$$\|\nabla\phi\|^2_{L^2(\Omega\setminus\mathsf{N}^m(T))} \leq \tilde{\beta}^{\lfloor m/5\rfloor}\|\nabla\phi\|^2_{L^2(\Omega)} \lesssim \tilde{\beta}^{\lfloor m/5\rfloor}\|\nabla v_H\|^2_{L^2(T)}.$$

This is the assertion. □

We proceed with the proof of Theorem 1.

Proof of Theorem 1. We define the cut-off function $\eta \in \mathcal{S}^1(\mathcal{G}_H)$ via

$$\eta \equiv 0 \quad \text{in } \Omega\setminus\mathsf{N}^{m-1}(T) \qquad \text{and} \qquad \eta \equiv 1 \quad \text{in } \mathsf{N}^{m-2}(T).$$

This function is thereby uniquely defined and satisfies the bound (A.2). Since $(1-I_H)I_h(\eta\mathcal{C}_{T,\infty}v) \in W_h(\Omega_T)$, we deduce with Céa's Lemma, the identity $I_H\mathcal{C}_{T,\infty}v = 0$ and the approximation and stability properties (3.1) and (A.1) and the resolution condition (4.3) that

$$\begin{aligned}
\|\nabla(\mathcal{C}_{T,\infty}v - \mathcal{C}_{T,m}v)\|^2_{L^2(\Omega)} &\lesssim \|\mathcal{C}_{T,\infty}v - (1-I_H)I_h(\eta\mathcal{C}_{T,\infty}v)\|^2_V \\
&= \|(1-I_H)I_h(\mathcal{C}_{T,\infty}v - \eta\mathcal{C}_{T,\infty}v)\|^2_{V,\Omega\setminus\{\eta=1\}} \\
&\lesssim \|\nabla(1-\eta)\mathcal{C}_{T,\infty}v\|^2_{L^2(\mathsf{N}(\Omega\setminus\{\eta=1\}))} \\
&\lesssim \|\nabla\mathcal{C}_{T,\infty}v\|^2_{L^2(\mathsf{N}(\Omega\setminus\{\eta=1\}))}.
\end{aligned}$$

Note that $\mathsf{N}(\Omega\setminus\{\eta=1\}) = \Omega\setminus\mathsf{N}^{m-3}(T)$. This and Theorem 4 prove (4.4).

Define $z := (\mathcal{C}_\infty - \mathcal{C}_m)v$ and $z_T := (\mathcal{C}_{T,\infty} - \mathcal{C}_{T,m})v$. The ellipticity from Lemma 1 proves

$$\frac{1}{2}\|\nabla z\|^2_{L^2(\Omega)} \leq \left|\sum_{T\in\mathcal{G}_H} a(z, z_T)\right|.$$

We define the cut-off function $\eta \in \mathcal{S}^1(\mathcal{G}_H)$ via

$$\eta \equiv 1 \quad \text{in } \Omega \setminus \mathsf{N}^{m+2}(T) \qquad \text{and} \qquad \eta \equiv 0 \quad \text{in } \mathsf{N}^{m+1}(T).$$

This function is thereby uniquely defined and satisfies the bound (A.2). For any $T \in \mathcal{G}_H$ we have $(1 - I_H)I_h(\eta z) \in W_h$ with support outside Ω_T. Hence, we obtain with $z = I_h z$ that

$$a(z, z_T) = a(I_h(z - \eta z), z_T) + a(I_H I_h(\eta z), z_T).$$

The function $z - I_h(\eta z)$ vanishes on $S := \{\eta = 1\}$. Hence, the first term on the right-hand side satisfies

$$|a(I_h(z - \eta z), z_T)| \leq C_a \|I_h(z - \eta z)\|_{V,\Omega\setminus S} \|z_T\|_V.$$

The Friedrichs inequality with constant C_{F} proves together with the stability (A.1) and the estimate (A.5) applied to the cut-off function $(1 - \eta)$ that

$$\|I_h(z - \eta z)\|_{V,\Omega\setminus S} \lesssim \sqrt{1 + (C_{\mathrm{F}}\kappa H)^2} \|\nabla z\|_{L^2(\Omega\setminus S)} \lesssim \|\nabla z\|_{L^2(\Omega\setminus S)}.$$

Furthermore, $I_H I_h(\eta z)$ vanishes on $\Omega \setminus \mathsf{N}(\mathrm{supp}(1 - \eta))$. Hence, we infer from Friedrichs' inequality and the resolution condition (4.3), the stability properties (3.1) and (A.1) and the (A.5) that

$$|a(z_T, I_H I_h(\eta z))| \lesssim \|\nabla z\|_{L^2(\mathsf{N}^2(\mathrm{supp}(1-\eta)))} \|z_T\|_V.$$

The sum over all $T \in \mathcal{G}_H$ and the Cauchy inequality yield with the finite overlap of patches

$$\begin{aligned} \|\nabla z\|^2_{L^2(\Omega)} &\lesssim \sum_{T\in\mathcal{G}_H} \|\nabla z\|_{L^2(\mathsf{N}^2(\mathrm{supp}(1-\eta)))} \|z_T\|_V \\ &\lesssim \sqrt{C_{\mathrm{ol},m}} \|\nabla z\|_{L^2(\Omega)} \sqrt{\sum_{T\in\mathcal{G}_H} \|z_T\|^2_V}. \end{aligned}$$

The combination with (4.4) concludes the proof. □

References

[BCWG+11] T. Betcke, S. N. Chandler-Wilde, I. G. Graham, S. Langdon, and M. Lindner. Condition number estimates for combined potential integral operators in acoustics and their boundary element discretisation. *Numer. Methods Partial Differential Equations*, 27(1):31–69, 2011.

[BP14] D. Brown and D. Peterseim. A multiscale method for porous microstructures. *ArXiv e-prints*, November 2014.

[BS00] I. M. Babuska and S. A. Sauter. Is the pollution effect of the FEM avoidable for the Helmholtz equation considering high wave numbers? *SIAM Rev.*, 42(3):451–484, 2000.

[CF06] P. Cummings and X. Feng. Sharp regularity coefficient estimates for complex-valued acoustic and elastic Helmholtz equations. *Math. Models Methods Appl. Sci.*, 16(1):139–160, 2006.

[DE12] D. A. Di Pietro and A. Ern. *Mathematical aspects of discontinuous Galerkin methods*, volume 69 of *Mathématiques & Applications (Berlin)*. Springer, Heidelberg, 2012.

[DGMZ12] L. Demkowicz, J. Gopalakrishnan, I. Muga, and J. Zitelli. Wavenumber explicit analysis of a DPG method for the multidimensional Helmholtz equation. *Comput. Methods Appl. Mech. Engrg.*, 213/216:126–138, 2012.

[EGMP13] D. Elfverson, E. H. Georgoulis, A. Målqvist, and D. Peterseim. Convergence of a discontinuous Galerkin multiscale method. *SIAM Journal on Numerical Analysis*, 51(6):3351–3372, 2013.

[EM12] S. Esterhazy and J. M. Melenk. On stability of discretizations of the Helmholtz equation. In *Numerical analysis of multiscale problems*, volume 83 of *Lect. Notes Comput. Sci. Eng.*, pages 285–324. Springer, Heidelberg, 2012.

[FW09] X. Feng and H. Wu. Discontinuous Galerkin methods for the Helmholtz equation with large wave number. *SIAM J. Numer. Anal.*, 47(4):2872–2896, 2009.

[FW11] X. Feng and H. Wu. *hp*-discontinuous Galerkin methods for the Helmholtz equation with large wave number. *Math. Comp.*, 80(276):1997–2024, 2011.

[Het07] U. Hetmaniuk. Stability estimates for a class of Helmholtz problems. *Commun. Math. Sci.*, 5(3):665–678, 2007.

[HFMQ98] T. J. R. Hughes, G. R. Feijóo, L. Mazzei, and J.-B. Quincy. The variational multiscale method—a paradigm for computational mechanics. *Comput. Methods Appl. Mech. Engrg.*, 166(1-2):3–24, 1998.

[HMP11] R. Hiptmair, A. Moiola, and I. Perugia. Plane wave discontinuous Galerkin methods for the 2D Helmholtz equation: analysis of the *p*-version. *SIAM J. Numer. Anal.*, 49(1):264–284, 2011.

[HMP14a] P. Henning, P. Morgenstern, and D. Peterseim. Multiscale Partition of Unity. In M. Griebel and M. A. Schweitzer, editors, *Meshfree Methods for Partial Differential Equations VII*, volume 100 of *Lecture Notes in Computational Science and Engineering*. Springer, 2014.

[HMP14b] R. Hiptmair, A. Moiola, and I. Perugia. Trefftz discontinuous Galerkin methods for acoustic scattering on locally refined meshes. *Appl. Numer. Math.*, 79:79–91, 2014.

[HP13] P. Henning and D. Peterseim. Oversampling for the multiscale finite element method. *Multiscale Modeling & Simulation*, 11(4):1149–1175, 2013.

[HS07] T. Hughes and G. Sangalli. Variational multiscale analysis: the fine-scale Green's function, projection, optimization, localization, and stabilized methods. *SIAM J. Numer. Anal.*, 45(2):539–557, 2007.

[Hug95] T. J. R. Hughes. Multiscale phenomena: Green's functions, the Dirichlet-to-Neumann formulation, subgrid scale models, bubbles and the origins of stabilized methods. *Comput. Methods Appl. Mech. Engrg.*, 127(1-4):387–401, 1995.

[Ihl98] Frank Ihlenburg. *Finite element analysis of acoustic scattering*, volume 132 of *Applied Mathematical Sciences*. Springer-Verlag, New York, 1998.

[Mål11] A. Målqvist. Multiscale methods for elliptic problems. *Multiscale Model. Simul.*, 9(3):1064–1086, 2011.

[Mel95] J. M. Melenk. *On generalized finite-element methods*. ProQuest LLC, Ann Arbor, MI, 1995. Thesis (Ph.D.)–University of Maryland, College Park.

[MIB96] Ch. Makridakis, F. Ihlenburg, and I. Babuška. Analysis and finite element methods for a fluid-solid interaction problem in one dimension. *Mathematical Models and Methods in Applied Sciences*, 06(08):1119–1141, 1996.

[MP14] A. Målqvist and D. Peterseim. Localization of elliptic multiscale problems. *Math. Comp.*, 83(290):2583–2603, 2014.

[MS10] J. M. Melenk and S. A. Sauter. Convergence analysis for finite element discretizations of the Helmholtz equation with Dirichlet-to-Neumann boundary conditions. *Math. Comp.*, 79(272):1871–1914, 2010.

[MS11a] J. M. Melenk and S. Sauter. Wavenumber explicit convergence analysis for Galerkin discretizations of the Helmholtz equation. *SIAM J. Numer. Anal.*, 49(3):1210–1243, 2011.

[MS11b] J. M. Melenk and S. A. Sauter. Wave-number explicit convergence analysis for Galerkin discretizations of the Helmholtz equation. *SIAM J. Numer. Anal.*, 49:1210–1243, 2011.

[Pet14] D. Peterseim. Eliminating the pollution effect in Helmholtz problems by local subscale correction. *ArXiv e-prints*, 1411.1944, 2014.

[Pet15] D. Peterseim. Variational multiscale stabilization and the exponential decay of fine-scale correctors. *ArXiv e-prints*, 1505.07611, 2015.

[TF06] R. Tezaur and C. Farhat. Three-dimensional discontinuous Galerkin elements with plane waves and Lagrange multipliers for the solution of mid-frequency Helmholtz problems. *Internat. J. Numer. Methods Engrg.*, 66(5):796–815, 2006.

[Wu14] H. Wu. Pre-asymptotic error analysis of CIP-FEM and FEM for the Helmholtz equation with high wave number. Part I: linear version. *IMA J. Numer. Anal.*, 34(3):1266–1288, 2014.

[ZMD+11] J. Zitelli, I. Muga, L. Demkowicz, J. Gopalakrishnan, D. Pardo, and V.M. Calo. A class of discontinuous Petrov–Galerkin methods. part IV: The optimal test norm and time-harmonic wave propagation in 1D. *Journal of Computational Physics*, 230(7):2406 – 2432, 2011.